Cancer Cell
Report

Innate Neural Stem Cell Heterogeneity Determines the Patterning of Glioma Formation in Children

Da Yong Lee,[1] Scott M. Gianino,[1] and David H. Gutmann[1,*]
[1]Department of Neurology, Washington University School of Medicine, St. Louis, MO 63110, USA
*Correspondence: gutmannd@wustl.edu
http://dx.doi.org/10.1016/j.ccr.2012.05.036

SUMMARY

The concept that gliomas comprise a heterogeneous group of diseases distinguished by their developmental origin raises the intriguing possibility that neural stem cells (NSCs) from different germinal zones have differential capacities to respond to glioma-causing genetic changes. We demonstrate that lateral ventricle subventricular zone NSCs are molecularly and functionally distinct from those of the third ventricle. Consistent with a unique origin for pediatric low-grade glioma, third ventricle, but not lateral ventricle, NSCs hyperproliferate in response to mutations characteristic of childhood glioma. Finally, we demonstrate that pediatric optic gliomas in *Nf1* genetically engineered mice arise from the third ventricle. Collectively, these observations establish the importance of innate brain region NSC heterogeneity in the patterning of gliomagenesis in children and adults.

INTRODUCTION

The importance of the cell of origin in tumorigenesis and clinical behavior of brain tumors (Singh et al., 2004; Taylor et al., 2005) has been strengthened by the observation that histologically identical brain tumors are composed of molecularly distinct subtypes that reflect their progenitor cell of origin (Gibson et al., 2010; Johnson et al., 2010; Kalamarides et al., 2011; Sharma et al., 2007). These findings suggest that brain tumors with distinct cellular origins are unique diseases with different growth control regulatory networks, genetic changes, and responses to therapy. Consistent with this, we have shown that mouse neural stem cells (NSCs) from the brainstem, but not the neocortex, exhibit increased proliferation and gliogenesis following inactivation of the neurofibromatosis-1 (NF1) tumor suppressor gene (Lee et al., 2010). This differential sensitivity to *Nf1* loss closely parallels the propensity for pilocytic astrocytomas (PAs) in children with NF1 to form within the optic pathway and brainstem, but rarely in the cortex (Guillamo et al., 2003). A similar geographic pattern of gliomagenesis is observed for sporadic pediatric PAs harboring *KIAA1549:BRAF* fusions (Jacob et al., 2009), which predominantly form in the cerebellum.

Within the brain there are several germinal zones potentially germane to brain tumorigenesis, including the subventricular zone of the lateral ventricle (lv-SVZ), the third ventricle (TVZ), and the fourth ventricle (Quiñones-Hinojosa et al., 2006; Weiss et al., 1996; Xu et al., 2005). Although the lv-SVZ is often considered to be the likely stem cell compartment for cerebral hemisphere glioma formation in mice following the introduction of genetic alterations observed in high-grade human adult gliomas (Alcantara Llaguno et al., 2009; Jacques et al., 2010; Wang et al., 2009), other populations, including $NG2^+$ cells (Assanah et al., 2006; Masui et al., 2010) and oligodendrocyte precursors (Liu et al., 2011; Sugiarto et al., 2011), can serve as potential cells of origin for malignant glioma. However, to our knowledge, the origin of optic glioma, the second-most common low-grade pediatric glioma, remains unresolved. Based on the proximity of the optic nerve/chiasm to the TVZ and that optic nerve oligodendrocyte precursors can originate from the TVZ (Ono et al., 1997), we hypothesized that TVZ may be the progenitor compartment for these pediatric brain tumors.

RESULTS

NSCs from the lv-SVZ and TVZ Are Molecularly Distinct Populations

We obtained several lines of evidence supporting that TVZ is a true stem cell niche. First, cells lining the TVZ in the embryonic

Significance

Whereas some adult malignant cerebral hemispheric gliomas have been shown to arise from neural stem or progenitor cells residing in the subventricular zone of the lateral ventricle (lv-SVZ), to our knowledge, the cellular origin of pediatric low-grade gliomas is unknown. Consistent with the propensity for childhood gliomas to develop in the optic nerve and chiasm, we demonstrate that third ventricle (TVZ) NSCs are molecularly and functionally distinct from their lv-SVZ counterparts and are the likely cell of origin for murine low-grade optic gliomas. These findings establish brain region NSC heterogeneity as a major determinant underlying the patterning of gliomagenesis in children and adults.

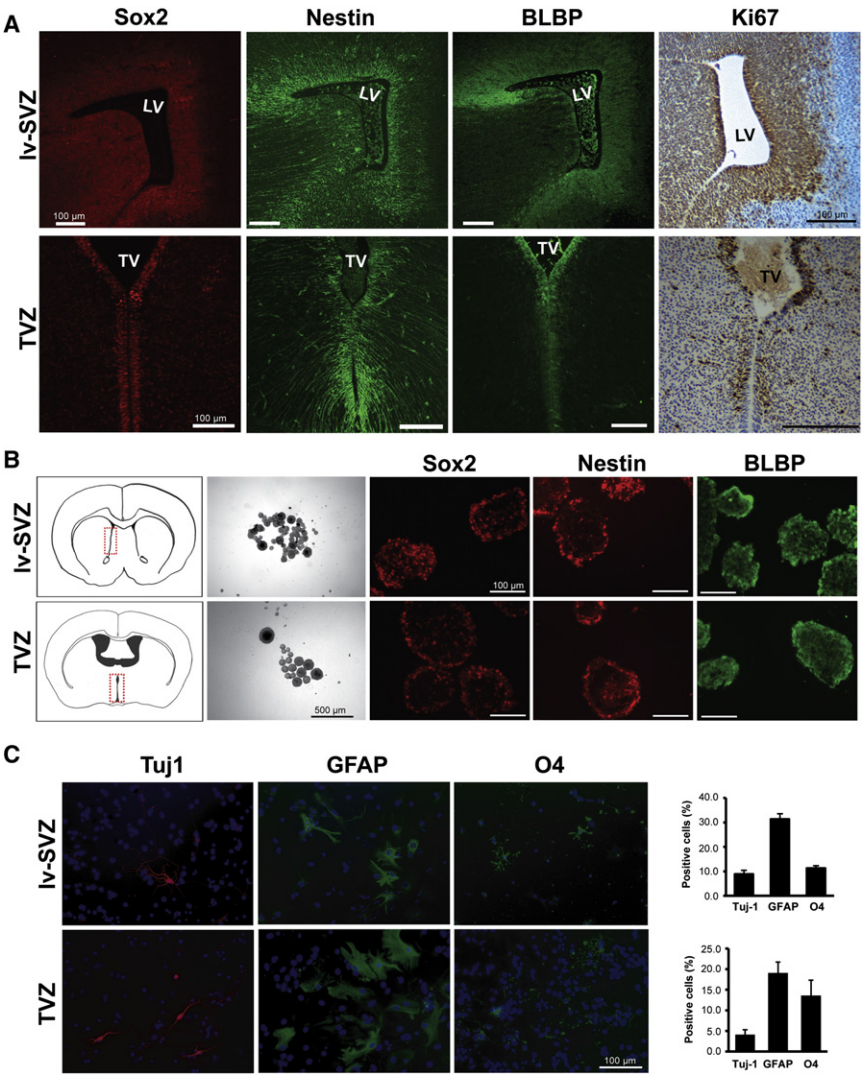

Figure 1. NSCs Can Be Generated from the lv-SVZ and TVZ

(A) Immunostaining of the cells lining the mouse E15.5 TVZ shows expression of the Sox2, nestin, and BLBP NSC markers. LV, lateral ventricle; TV, third ventricle.

(B) Single neurospheres from the lv-SVZ and TVZ form secondary neurospheres in vitro and express Sox2, nestin, and BLBP. The diagrams denote the regions used for NSC cultures.

(C) TVZ NSCs can differentiate into neurons (Tuj-1), astrocytes (GFAP), and oligodendrocytes (O4). Values denote the mean ± SEM.

Scale bars: (A) and (C), 100 μm; (B) phase contrast, 500 μm; (B) fluorescence, 100 μm.

day 15.5 (E15.5) mouse brain express NSC markers Sox2, nestin, and BLBP, and exhibit robust proliferation (Ki67 immunostaining) (Figure 1A). Second, TVZ NSCs can generate Sox2$^+$, nestin$^+$, and BLBP$^+$ neurospheres and undergo self-renewal, similar to their lv-SVZ counterparts (Figure 1B). Third, dissociated single cells from TVZ neurospheres differentiate into neurons, astrocytes, and oligodendrocytes in vitro (Figure 1C).

We then employed gene expression profiling to demonstrate that TVZ NSCs and lv-SVZ NSCs are molecularly distinct populations. Initially, E17.5 TVZ and lv-SVZ NSCs from three females were used for the profiling; however, one outlier lv-SVZ NSC sample, based on principal component analysis (PCA), was eliminated from the following analyses (see Figure S1A available online). Using hierarchical clustering methods, lv-SVZ and TVZ NSCs were easily separable (Figures 2A and S1A). The differential expression of several genes was validated by quantitative reverse-transcription PCR (Figure 2B) and by in situ hybridization (Allen Brain Atlas at http://www.brain-map.org/): *Chl1* and *Slit2* expression was higher in the hypothalamus/TVZ region compared to the anterior forebrain/lv-SVZ region, whereas *Dcx* and *Cntn1* expression was higher in the anterior forebrain/lv-SVZ region relative to the hypothalamus/TVZ region (Figure S1B). A subset of these genes was also similarly differentially expressed in older mice (Figures S1B and S1C). Together, these data demonstrate that TVZ and lv-SVZ contain molecularly distinct NSC populations.

lv-SVZ and TVZ NSCs Exhibit Unique Cell-Autonomous Responses to Glioma-Causing Genetic Mutations

To determine whether TVZ and lv-SVZ NSCs exhibit different responses to glioma-associated genetic events, we measured NSC proliferation in response to *KIAA1549:BRAF* expression, a representative pediatric glioma-causing genetic change (Jones et al., 2008), *PTEN* loss, a representative adult glioma-causing genetic change (Pollack et al., 2006), and *p53* loss, which occurs in both adult and pediatric gliomas (Hayes et al., 1999; Kim et al., 2010). The *KIAA1549:BRAF* mutation is found in 62% of hypothalamus/optic pathway PAs but is uncommon in histologically identical tumors of the cerebral hemispheres (14%) (Jacob et al., 2009). *p53* inactivation increased proliferation and decreased apoptosis of both lv-SVZ and TVZ NSCs (Figure 2C, top, and Figure S1D). *Pten* inactivation increased proliferation of lv-SVZ, but not in TVZ, NSCs, whereas *KIAA1549:BRAF* overexpression increased proliferation of TVZ, but not in lv-SVZ, NSCs, with no effect in apoptosis (Figures 2C and S1D). Decreased apoptosis was observed in both NSC populations following *Pten* loss, whereas *KIAA1549:BRAF* overexpression resulted in no change. These differential responses do not reflect a failure to activate AKT following *Pten* loss in TVZ NSCs or MEK following *KIAA1549:BRAF* expression in lv-SVZ NSCs (Figure S1E).

Mouse Nf1 Optic Gliomas Arise from TVZ

To identify the ventricular zone of origin for optic glioma, we chose NF1 as a model experimental system because gliomas

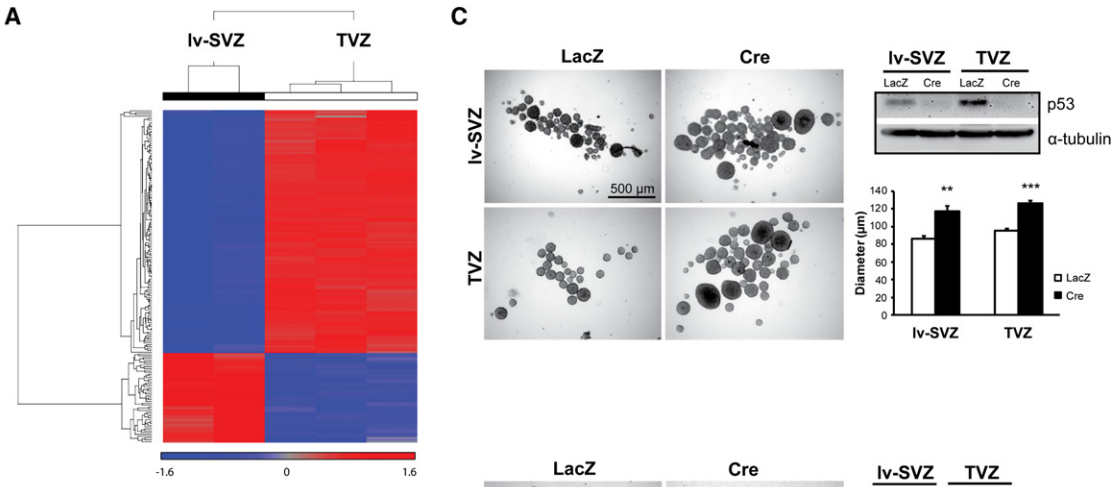

B

Gene Symbol	Microarray FC (TVZ/lv-SVZ)	Microarray p	q-PCR FC (TVZ/lv-SVZ)	q-PCR p
Casc5	3.76268	0.00396	5.17	<0.0001
Chl1	6.07247	0.011865	11.41	0.0333
Ect2	4.20363	0.009195	11.09	0.0005
Fignl1	4.22097	0.007586	5.58	0.0091
Gmnn	3.49677	0.006895	7.73	<0.0001
Hmmr	4.37526	0.001085	3.5	0.0081
Nr2f2	3.73674	0.004442	4.51	0.0064
Pbk	4.25061	0.007103	6.04	0.0008
Shcbp1	3.90795	0.012452	9.24	0.0005
Slit2	3.3639	0.000299	3.36	0.0046
Ttk	4.25887	0.006919	13.61	0.0027

Gene Symbol	Microarray FC (lv-SVZ/TVZ)	Microarray p	q-PCR FC (lv-SVZ/TVZ)	q-PCR p
Apoe	4.12505	0.007103	4.55716	0.0446
Cntn1	4.21629	0.009195	4.08644	0.0013
Dcx	3.77764	0.022158	22.5876	0.0071
Gng3	5.64923	0.000731	2.88	0.0069
Ptsg2	4.8974	0.007586	3.04273	0.0045
Rbp1	14.0755	0.00004	7.14286	0.0032

Figure 2. NSCs from the lv-SVZ and TVZ Are Molecularly Distinct Progenitor Populations with Unique Cell-Autonomous Responses to Glioma-Causing Genetic Mutations

(A) SAM separates lv-SVZ and TVZ NSCs with the expression level represented as standardized values from −1.6 (blue, <1-fold change) to 1.6 (red, >1-fold change). No change (0 value) is denoted by gray.

(B) Validation of select differentially expressed transcripts by quantitative reverse-transcription PCR with fold changes (FC) and p values (p) are shown.

(C) Increased neurosphere diameters were observed in NSCs from both the lv-SVZ and TVZ following *p53* loss. Increased neurosphere diameters were found only in lv-SVZ NSCs following *Pten* loss. Increased neurosphere diameters were observed only in TVZ NSCs following *KIAA1549:BRAF* expression (RT-PCR). Values denote the mean ± SEM. $p^* < 0.01$, $p^{**} < 0.001$, $p^{***} < 0.0001$.

Scale bars, 500 μm.

See also Figure S1.

predominate in the optic pathway of children with this syndrome (Guillamo et al., 2003). Similar to human NF1-associated gliomas, optic gliomas form in the prechiasmatic and chiasmal regions of $Nf1^{+/-}$ mice following complete *Nf1* inactivation in glial progenitors (Figure 3A) (Bajenaru et al., 2003). These gliomas could arise from NSCs in the lv-SVZ, TVZ (Figure 3B), optic nerve, or retina.

We first excluded the retina and optic nerve as cell of origin of these gliomas because true NSCs capable of self-renewal and multilineage differentiation could not be generated from either E17.5 or postnatal day (P) 1 retina cells or the optic nerve (Figure S2A; Cicero et al., 2009; Lee et al., 2010). Additionally, Cre transgene expression ($LacZ^+$ cells) was not detected in the retina

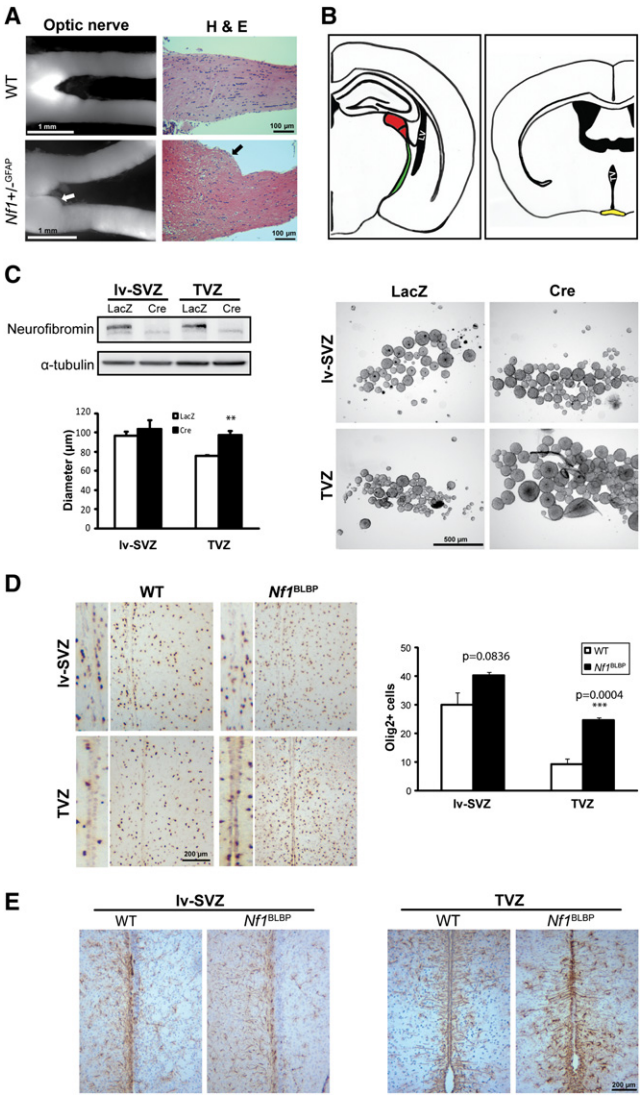

Figure 3. TVZ NSCs Are Preferentially Sensitive to *Nf1* Loss

(A) Increased optic nerve volume (white arrow) and abnormal cell clusters (black arrow) were observed in optic gliomas from 3-month-old $Nf1^{+/-GFAP}$ mice. H&E, hematoxylin and eosin staining; WT, wild-type.

(B) The potential cellular origins (lv-SVZ and TVZ) of optic gliomas in *Nf1* mutant mice are illustrated. Lateral ventricle (LV) is shown in black, lateral geniculate nucleus in red, third ventricle (TV) in black, optic tract in green, and optic chiasm in yellow.

(C) Increased TVZ neurosphere proliferation was seen following *Nf1* loss, with little effect on lv-SVZ NSCs.

(D) There were 3-fold more $Olig2^+$ cells found in the TVZ of $Nf1^{BLBP}$ mice ($p = 0.0004$), but not in the lv-SVZ ($p = 0.0836$), compared to controls.

(E) Increased numbers of $GFAP^+$ cells were found in the TVZ, but not in the lv-SVZ, of $Nf1^{BLBP}$ mice compared to controls.

Values denote the mean ± SEM. Scale bars: (A) left, 1 mm; (A) right, 100 μm; (C), 500 μm; (D) and (E), 200 μm.

See also Figure S2.

or optic nerve until after P2 or E17.5, respectively (Figure S2B). We then show that $Nf1^{-/-}$ NSCs from the TVZ, but not the lv-SVZ, exhibit increased proliferation relative to wild-type NSCs, with no effect on apoptosis in vitro (Figures 3C and S2C).

To provide in vivo support for these in vitro observations, we inactivated *Nf1* in $BLBP^+$ NSCs beginning at E9.5 and found that the numbers of $Olig2^+$ glial progenitors (Figure 3D) and $GFAP^+$ astrocytes (Figure 3E) were increased in the TVZ, but not in the lv-SVZ, of P8 $Nf1^{BLBP}$ mice compared to control littermates in vivo.

To examine whether human hypothalamic/optic gliomas recapitulate the gene expression pattern of TVZ (Sharma et al., 2007), PCA and hierarchical clustering revealed that hypothalamic/optic pathway gliomas were separated from their supratentorial counterparts (Figure S2D). Although some of the differentially expressed genes were not represented on the human Affymetrix Gene Chip, we found that one differentially expressed TVZ transcript (*Slit2*) was significantly higher (3.7-fold; $p = 0.001$) in hypothalamic/optic PAs compared to supratentorial PAs. Two other TVZ-overexpressed transcripts (*Gmnn* and *Nr2f2*) and two lv-SVZ-overexpressed transcripts (*Cntn1* and *Apoe*) also exhibited increased expression in hypothalamic/optic gliomas and supratentorial gliomas, respectively, although not reaching statistical significance, likely due to the small sample size ($p = 0.08–0.1$) (Figure S2D).

Finally, we sought to define a developmental window when optic glioma formation is favored by virtue of the selective proliferative activity of the TVZ and lv-SVZ using three different GFAP-Cre driver lines with distinct patterns of Cre-mediated *Nf1* inactivation in vivo (Figures S3A and 4A). The *GFAP-Cre:IRES-LacZ* strain used to generate $Nf1^{+/-GFAP}$ mouse optic gliomas has detectable LacZ expression in the lv-SVZ and TVZ beginning at E15.5 (Figure 4B). The GFAP-Cre* strain (Zhuo et al., 2001) initiates Cre expression in the anterior part of forebrain by E13.5 (Figures 4A and 4C) and in the hypothalamus, which includes the TVZ, by E16.5 (Figure 4C). $Nf1^{+/-GFAP^*}$ mice also develop optic glioma (Zhu et al., 2005) (Figure 4E). Analysis of the TVZ and lv-SVZ in these mice reveals that $nestin^+$ and $Ki67^+$ progenitor cells reside in both germinal zones at E15.5 (Figure 4B).

To distinguish between these two germinal zones, we employed the GFAP-Cre^{ER} strain, which was similar to the first GFAP-Cre strain, but expressed a tamoxifen-regulatable Cre (Cre^{ER}; Chow et al., 2008). Recombination and inactivation of the *Nf1* gene were verified by recombination PCR (Figure 4D), whereas Cre activity in the brain, optic chiasm, and optic nerve following tamoxifen injection was demonstrated using ROSA-GREEN reporter mice (Figure 4D). Because lv-SVZ contained $nestin^+$ $Ki67^+$ cells at P8–P14, whereas these proliferating progenitors disappeared after P2 in TVZ (Figures 4B, S3B, and S3C), we inactivated *Nf1* either during the first postnatal week of life (P1–P3) or at 2 weeks of age when only the lv-SVZ harbors significant numbers of proliferating ($Ki67^+$) progenitor ($nestin^+$) cells (Figures S3B and S3C). *Nf1* loss at these times did not result in glioma formation at 3 months of age (Figure 4E). As an internal control for the fidelity of the GFAP-Cre^{ER} strain for inducing optic glioma, we treated >20 litters of pregnant females with tamoxifen at E16.5 (50 μg/g i.p.). The vast majority of pregnant dams did not deliver viable mice; however, the one embryonically treated pup that survived to 3 months of age developed an optic glioma (Figure S3D) with increased numbers of $Ki67^+$ cells and increased numbers of $GFAP^+$ astrocytes (Figure S3E). Taken together, these data establish that optic gliomas arise from neural stem/progenitor cells in the proliferative TVZ during

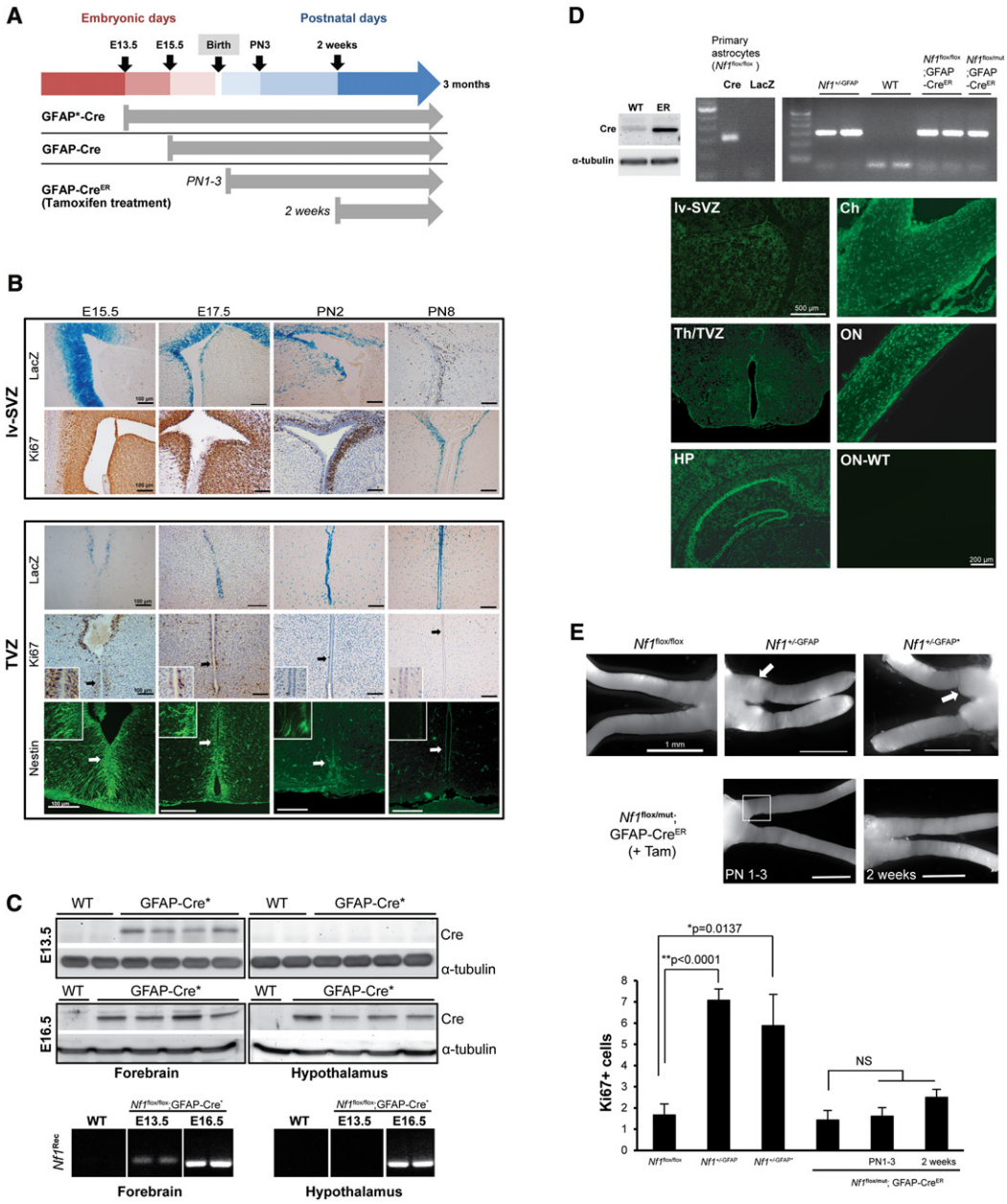

Figure 4. Embryonic *Nf1* Inactivation Is Required for Optic Glioma Formation

(A) The timing of *Nf1* inactivation by Cre-mediated excision is shown for each strain.

(B) X-Gal staining reveals GFAP-Cre transgene expression in the lv-SVZ and TVZ beginning at E15.5. Whereas lv-SVZ cells are Ki67$^+$ from E15.5 through P8, scant numbers of Ki67$^+$ or nestin$^+$ cells are detected in the TVZ by P2.

(C) Cre expression and *Nf1* gene recombination (*Nf1*^{Rec}) are detected by E13.5 in the anterior forebrain/lv-SVZ ("forebrain") and by E16.5 in the hypothalamus/TVZ ("hypothalamus") of GFAP-Cre* mice.

(D) Cre-mediated *Nf1* gene recombination (PCR) in *Nf1*$^{+/-GFAP}$ mice and in tamoxifen-treated *Nf1*$^{flox/flox}$; GFAP-Cre^{ER} and *Nf1*$^{flox/mut}$; GFAP-Cre^{ER} mice was seen. Wild-type (WT) C57BL/6 mouse brain was used as a negative control, whereas Ad5Cre-infected (Cre) and Ad5LacZ-infected (LacZ) *Nf1*$^{flox/flox}$ astrocytes served as positive and WT controls, respectively. Cre-ER fusion protein (~70 kDa) expression was detected in GFAP-Cre^{ER} (ER), but not in WT, mouse brains. EGFP was expressed in tamoxifen-treated ROSA-GREEN; GFAP-Cre^{ER} mouse brains and optic nerves (ON) at 1 month of age, but not in a WT mouse optic nerve (ON-WT). HP, hippocampus; Th, thalamus; Ch, chiasm.

(E) Whereas optic gliomas develop in *Nf1*$^{+/-GFAP}$ and *Nf1*$^{+/-GFAP^*}$ mice, no gliomas formed in *Nf1*$^{flox/flox}$ or *Nf1*$^{flox/mut}$; GFAP-Cre^{ER} treated with tamoxifen (+Tam) beginning at P1 or P14. Increased Ki67$^+$ cells were found in the prechiasmatic and chiasmal regions (square) of *Nf1*$^{+/-GFAP}$ and *Nf1*$^{+/-GFAP^*}$ mice. In contrast, the number of Ki67$^+$ cells in *Nf1*$^{flox/mut}$; GFAP-Cre^{ER} postnatally treated with tamoxifen is indistinguishable from control *Nf1*$^{flox/flox}$ mice. Values denote the mean ± SEM. NS, not significant.

Scale bars: (B), 100 μm; (D) left, 500 μm; (D) right, 200 μm; (E), 1 mm. PN, postnatal days.

See also Figure S3.

embryogenesis rather than from astrocytes at later postnatal stages.

DISCUSSION

Our finding that NSCs from two different germinal zones are molecularly distinct stem cell populations is consistent with previous reports examining mouse embryonic spinal cord and brain NSCs as well as human neural progenitor cells from the developing cortex and ventral midbrain (Johnson et al., 2010; Kelly et al., 2009; Kim et al., 2009; Taylor et al., 2005). In each case the unique genetic signature reflects the regional identity of the progenitors. Importantly, we show that the heterogeneity revealed at the molecular level translates into unique functional responses to glioma-causing genetic changes seen in children and adults. Although, to our knowledge, the precise etiologies for these innate differences are unknown, they likely reflect transcriptional networks and signaling set points unique to these brain regions. For example we have previously shown that the expression of the mTOR component rictor underlies the ability of *Nf1*-deficient NSCs to increase their proliferation and glial differentiation (Lee et al., 2010), whereas basal cAMP levels in specific brain regions partly dictate the spatial pattern of gliomagenesis in NF1 (Warrington et al., 2010).

We also provide several lines of converging evidence that optic gliomas likely originate from stem/progenitor cells residing in the TVZ. Although both TVZ and lv-SVZ germinal zones could provide cells of origin for these tumors, only TVZ, but not lv-SVZ, NSCs exhibit increased proliferation and gliogenesis following *Nf1* inactivation. In addition, optic gliomas do not form in mouse strains following postnatal *Nf1* inactivation when only lv-SVZ NSCs are proliferating. These latter experiments also demonstrate that *Nf1* inactivation in GFAP-expressing astrocytes in young mice does not result in optic gliomagenesis. One report employing immunohistochemical and gene expression analysis similarly suggested that human optic gliomas might derive from third ventricle glial progenitors (Tchoghandjian et al., 2009). This result parallels the developmental origins of another optic nerve glial cell population in which oligodendrocyte precursor cells generated in the floor of the TVZ differentiate and migrate into the optic nerve in response to signaling molecules from retinal ganglion axons (Gao and Miller, 2006; Ono et al., 1997).

Although our mouse experimental data argue that optic gliomas in children with NF1 arise from the TVZ, it is possible that we have modeled only one type of human optic glioma, and that other subtypes of optic glioma originate from different progenitor cells akin to other CNS cancers (Gibson et al., 2010; Johnson et al., 2010). Additional potential progenitors could be $NG2^+$ oligodendrocyte precursor cells recently implicated in malignant gliomagenesis (Assanah et al., 2006; Liu et al., 2011; Masui et al., 2010; Sugiarto et al., 2011). However, *Nf1* inactivation in $NG2^+$ cells of $Nf1^{+/-}$ mice, similar to the *Nf1* mouse models described here, is not sufficient for glioma formation (A. Solga, unpublished data). Future studies aimed at subdividing these common pediatric tumors into molecularly distinct diseases will facilitate the development of brain tumor therapies targeted to the specific growth regulatory pathways that drive cell growth and differentiation in these distinct cancer-initiating cell populations.

EXPERIMENTAL PROCEDURES

Mice

All strains were generated (Supplemental Experimental Procedures), maintained on a C57BL/6 background, and used under an approved Animal Studies Committee protocol at Washington University.

NSC Isolation and Analysis

lv-SVZ and TVZ NSCs from $Nf1^{flox/flox}$, $p53^{flox/flox}$, and $Pten^{flox/flox}$ P1 mouse pups were infected with adenovirus containing LacZ or Cre, and protein loss was confirmed by western blotting (Lee et al., 2010). NSCs expressing *KIAA1549:BRAF* were generated following retrovirus infection (Peter Collins, University of Cambridge) and verified by RT-PCR (Supplemental Experimental Procedures). pBABE-puro retrovirus was used as control. NSC proliferation and multilineage differentiation assays were performed as described previously by Lee et al. (2010).

Immunohistochemistry and Immunocytochemistry

Tissues and cells were prepared as previously reported by Hegedus et al. (2007) prior to staining with appropriate antibodies (Supplemental Experimental Procedures).

Microarray Analysis

RNA from three independent litters of E17.5 C57BL/6 lv-SVZ and TVZ NSCs was subjected to microarray profiling (Supplemental Experimental Procedures), and differentially expressed probe sets ($p < 0.05$; fold change >3-fold increase or decrease) were prioritized for validation.

Quantitative Reverse-Transcription PCR

mRNA expression was determined by quantitative reverse-transcription PCR using NSCs from independently generated litters as described previously by Yeh et al. (2009) (Supplemental Experimental Procedures).

X-Gal Staining

Six micrometer frozen sections were stained with X-Gal (Gold Biotechnology, St. Louis) (Hegedus et al., 2007).

Tamoxifen Injection and Recombination PCR

Tamoxifen was injected into lactating females (1 mg/50 μl i.p.) at P1–P3 or P14–P18 (Supplemental Experimental Procedures), and *Nf1* recombination was determined by recombination PCR (Mayes et al., 2011).

Western Blotting

Western blotting was performed as reported previously by Lee et al. (2010) (Supplemental Experimental Procedures).

Statistical Analyses

Each experiment was performed with samples from at least three independent litters. Statistical significance ($p < 0.05$) was determined (Student's t test) using GraphPad Prism 5.0 software (GraphPad).

ACCESSION NUMBERS

Human PA (GSE5675) and mouse NSC (GSE37832) microarray data were deposited in the Gene Expression Omnibus (http://www.ncbi.nlm.nih.gov/geo/).

SUPPLEMENTAL INFORMATION

Supplemental Information includes three figures, Supplemental Experimental Procedures, and Supplemental Referneces and can be found with this article online at http://dx.doi.org/10.1016/j.ccr.2012.05.036.

ACKNOWLEDGMENTS

We thank Crystal White-Worsena and Madelyn Reynolds for technical assistance and Suzanne Baker (St. Jude Children's Research Hospital, Memphis,

TN) for the GFAP-Cre^{ER} mice. This work was funded by grants from the NIH (NS065547-01 to D.H.G.), NCI (CA141549-01 to D.H.G.), and the NEI (EY02687).

Received: December 8, 2011
Revised: April 7, 2012
Accepted: May 31, 2012
Published: July 9, 2012

REFERENCES

Alcantara Llaguno, S., Chen, J., Kwon, C.H., Jackson, E.L., Li, Y., Burns, D.K., Alvarez-Buylla, A., and Parada, L.F. (2009). Malignant astrocytomas originate from neural stem/progenitor cells in a somatic tumor suppressor mouse model. Cancer Cell *15*, 45–56.

Assanah, M., Lochhead, R., Ogden, A., Bruce, J., Goldman, J., and Canoll, P. (2006). Glial progenitors in adult white matter are driven to form malignant gliomas by platelet-derived growth factor-expressing retroviruses. J. Neurosci. *26*, 6781–6790.

Bajenaru, M.L., Hernandez, M.R., Perry, A., Zhu, Y., Parada, L.F., Garbow, J.R., and Gutmann, D.H. (2003). Optic nerve glioma in mice requires astrocyte Nf1 gene inactivation and Nf1 brain heterozygosity. Cancer Res. *63*, 8573–8577.

Chow, L.M., Zhang, J., and Baker, S.J. (2008). Inducible Cre recombinase activity in mouse mature astrocytes and adult neural precursor cells. Transgenic Res. *17*, 919–928.

Cicero, S.A., Johnson, D., Reyntjens, S., Frase, S., Connell, S., Chow, L.M., Baker, S.J., Sorrentino, B.P., and Dyer, M.A. (2009). Cells previously identified as retinal stem cells are pigmented ciliary epithelial cells. Proc. Natl. Acad. Sci. USA *106*, 6685–6690.

Gao, L., and Miller, R.H. (2006). Specification of optic nerve oligodendrocyte precursors by retinal ganglion cell axons. J. Neurosci. *26*, 7619–7628.

Gibson, P., Tong, Y., Robinson, G., Thompson, M.C., Currle, D.S., Eden, C., Kranenburg, T.A., Hogg, T., Poppleton, H., Martin, J., et al. (2010). Subtypes of medulloblastoma have distinct developmental origins. Nature *468*, 1095–1099.

Guillamo, J.S., Créange, A., Kalifa, C., Grill, J., Rodriguez, D., Doz, F., Barbarot, S., Zerah, M., Sanson, M., Bastuji-Garin, S., and Wolkenstein, P.; Réseau NF France. (2003). Prognostic factors of CNS tumours in Neurofibromatosis 1 (NF1): a retrospective study of 104 patients. Brain *126*, 152–160.

Hayes, V.M., Dirven, C.M., Dam, A., Verlind, E., Molenaar, W.M., Mooij, J.J., Hofstra, R.M., and Buys, C.H. (1999). High frequency of TP53 mutations in juvenile pilocytic astrocytomas indicates role of TP53 in the development of these tumors. Brain Pathol. *9*, 463–467.

Hegedus, B., Dasgupta, B., Shin, J.E., Emnett, R.J., Hart-Mahon, E.K., Elghazi, L., Bernal-Mizrachi, E., and Gutmann, D.H. (2007). Neurofibromatosis-1 regulates neuronal and glial cell differentiation from neuroglial progenitors in vivo by both cAMP- and Ras-dependent mechanisms. Cell Stem Cell *1*, 443–457.

Jacob, K., Albrecht, S., Sollier, C., Faury, D., Sader, E., Montpetit, A., Serre, D., Hauser, P., Garami, M., Bognar, L., et al. (2009). Duplication of 7q34 is specific to juvenile pilocytic astrocytomas and a hallmark of cerebellar and optic pathway tumours. Br. J. Cancer *101*, 722–733.

Jacques, T.S., Swales, A., Brzozowski, M.J., Henriquez, N.V., Linehan, J.M., Mirzadeh, Z., O' Malley, C., Naumann, H., Alvarez-Buylla, A., and Brandner, S. (2010). Combinations of genetic mutations in the adult neural stem cell compartment determine brain tumour phenotypes. EMBO J. *29*, 222–235.

Johnson, R.A., Wright, K.D., Poppleton, H., Mohankumar, K.M., Finkelstein, D., Pounds, S.B., Rand, V., Leary, S.E., White, E., Eden, C., et al. (2010). Cross-species genomics matches driver mutations and cell compartments to model ependymoma. Nature *466*, 632–636.

Jones, D.T., Kocialkowski, S., Liu, L., Pearson, D.M., Bäcklund, L.M., Ichimura, K., and Collins, V.P. (2008). Tandem duplication producing a novel oncogenic BRAF fusion gene defines the majority of pilocytic astrocytomas. Cancer Res. *68*, 8673–8677.

Kalamarides, M., Stemmer-Rachamimov, A.O., Niwa-Kawakita, M., Chareyre, F., Taranchon, E., Han, Z.Y., Martinelli, C., Lusis, E.A., Hegedus, B., Gutmann, D.H., and Giovannini, M. (2011). Identification of a progenitor cell of origin capable of generating diverse meningioma histological subtypes. Oncogene *30*, 2333–2344.

Kelly, T.K., Karsten, S.L., Geschwind, D.H., and Kornblum, H.I. (2009). Cell lineage and regional identity of cultured spinal cord neural stem cells and comparison to brain-derived neural stem cells. PLoS One *4*, e4213.

Kim, H.J., McMillan, E., Han, F., and Svendsen, C.N. (2009). Regionally specified human neural progenitor cells derived from the mesencephalon and forebrain undergo increased neurogenesis following overexpression of ASCL1. Stem Cells *27*, 390–398.

Kim, Y.H., Nobusawa, S., Mittelbronn, M., Paulus, W., Brokinkel, B., Keyvani, K., Sure, U., Wrede, K., Nakazato, Y., Tanaka, Y., et al. (2010). Molecular classification of low-grade diffuse gliomas. Am. J. Pathol. *177*, 2708–2714.

Lee, Y., Yeh, T.H., Emnett, R.J., White, C.R., and Gutmann, D.H. (2010). Neurofibromatosis-1 regulates neuroglial progenitor proliferation and glial differentiation in a brain region-specific manner. Genes Dev. *24*, 2317–2329.

Liu, C., Sage, J.C., Miller, M.R., Verhaak, R.G., Hippenmeyer, S., Vogel, H., Foreman, O., Bronson, R.T., Nishiyama, A., Luo, L., and Zong, H. (2011). Mosaic analysis with double markers reveals tumor cell of origin in glioma. Cell *146*, 209–221.

Masui, K., Suzuki, S.O., Torisu, R., Goldman, J.E., Canoll, P., and Iwaki, T. (2010). Glial progenitors in the brainstem give rise to malignant gliomas by platelet-derived growth factor stimulation. Glia *58*, 1050–1065.

Mayes, D.A., Rizvi, T.A., Cancelas, J.A., Kolasinski, N.T., Ciraolo, G.M., Stemmer-Rachamimov, A.O., and Ratner, N. (2011). Perinatal or adult Nf1 inactivation using tamoxifen-inducible PlpCre each cause neurofibroma formation. Cancer Res. *71*, 4675–4685.

Ono, K., Yasui, Y., Rutishauser, U., and Miller, R.H. (1997). Focal ventricular origin and migration of oligodendrocyte precursors into the chick optic nerve. Neuron *19*, 283–292.

Pollack, I.F., Hamilton, R.L., James, C.D., Finkelstein, S.D., Burnham, J., Yates, A.J., Holmes, E.J., Zhou, T., and Finlay, J.L.; Children's Oncology Group. (2006). Rarity of PTEN deletions and EGFR amplification in malignant gliomas of childhood: results from the Children's Cancer Group 945 cohort. J. Neurosurg. Suppl. *105*, 418–424.

Quiñones-Hinojosa, A., Sanai, N., Soriano-Navarro, M., Gonzalez-Perez, O., Mirzadeh, Z., Gil-Perotin, S., Romero-Rodriguez, R., Berger, M.S., Garcia-Verdugo, J.M., and Alvarez-Buylla, A. (2006). Cellular composition and cytoarchitecture of the adult human subventricular zone: a niche of neural stem cells. J. Comp. Neurol. *494*, 415–434.

Sharma, M.K., Mansur, D.B., Reifenberger, G., Perry, A., Leonard, J.R., Aldape, K.D., Albin, M.G., Emnett, R.J., Loeser, S., Watson, M.A., et al. (2007). Distinct genetic signatures among pilocytic astrocytomas relate to their brain region origin. Cancer Res. *67*, 890–900.

Singh, S.K., Hawkins, C., Clarke, I.D., Squire, J.A., Bayani, J., Hide, T., Henkelman, R.M., Cusimano, M.D., and Dirks, P.B. (2004). Identification of human brain tumour initiating cells. Nature *432*, 396–401.

Sugiarto, S., Persson, A.I., Munoz, E.G., Waldhuber, M., Lamagna, C., Andor, N., Hanecker, P., Ayers-Ringler, J., Phillips, J., Siu, J., et al. (2011). Asymmetry-defective oligodendrocyte progenitors are glioma precursors. Cancer Cell *20*, 328–340.

Taylor, M.D., Poppleton, H., Fuller, C., Su, X., Liu, Y., Jensen, P., Magdaleno, S., Dalton, J., Calabrese, C., Board, J., et al. (2005). Radial glia cells are candidate stem cells of ependymoma. Cancer Cell *8*, 323–335.

Tchoghandjian, A., Fernandez, C., Colin, C., El Ayachi, I., Voutsinos-Porche, B., Fina, F., Scavarda, D., Piercecchi-Marti, M.D., Intagliata, D., Ouafik, L., et al. (2009). Pilocytic astrocytoma of the optic pathway: a tumour deriving from radial glia cells with a specific gene signature. Brain *132*, 1523–1535.

Wang, Y., Yang, J., Zheng, H., Tomasek, G.J., Zhang, P., McKeever, P.E., Lee, E.Y., and Zhu, Y. (2009). Expression of mutant p53 proteins implicates a lineage relationship between neural stem cells and malignant astrocytic glioma in a murine model. Cancer Cell *15*, 514–526.

Warrington, N.M., Gianino, S.M., Jackson, E., Goldhoff, P., Garbow, J.R., Piwnica-Worms, D., Gutmann, D.H., and Rubin, J.B. (2010). Cyclic AMP suppression is sufficient to induce gliomagenesis in a mouse model of neurofibromatosis-1. Cancer Res. *70*, 5717–5727.

Weiss, S., Dunne, C., Hewson, J., Wohl, C., Wheatley, M., Peterson, A.C., and Reynolds, B.A. (1996). Multipotent CNS stem cells are present in the adult mammalian spinal cord and ventricular neuroaxis. J. Neurosci. *16*, 7599–7609.

Xu, Y., Tamamaki, N., Noda, T., Kimura, K., Itokazu, Y., Matsumoto, N., Dezawa, M., and Ide, C. (2005). Neurogenesis in the ependymal layer of the adult rat 3rd ventricle. Exp. Neurol. *192*, 251–264.

Yeh, T.H., Lee da, Y., Gianino, S.M., and Gutmann, D.H. (2009). Microarray analyses reveal regional astrocyte heterogeneity with implications for neurofibromatosis type 1 (NF1)-regulated glial proliferation. Glia *57*, 1239–1249.

Zhu, Y., Harada, T., Liu, L., Lush, M.E., Guignard, F., Harada, C., Burns, D.K., Bajenaru, M.L., Gutmann, D.H., and Parada, L.F. (2005). Inactivation of NF1 in CNS causes increased glial progenitor proliferation and optic glioma formation. Development *132*, 5577–5588.

Zhuo, L., Theis, M., Alvarez-Maya, I., Brenner, M., Willecke, K., and Messing, A. (2001). hGFAP-cre transgenic mice for manipulation of glial and neuronal function in vivo. Genesis *31*, 85–94.